Eur. Phys. J. B **31**, 29–39 (2003)
DOI: 10.1140/epjb/e2003-00005-y

THE EUROPEAN PHYSICAL JOURNAL B

Numerical results for ground states of spin glasses on Bethe lattices

S. Boettcher[a]

Physics Department, Emory University, Atlanta, Georgia 30322, USA

Received 9 August 2002
Published online 27 January 2003 –

Abstract. The average ground state energy and entropy for $\pm J$ spin glasses on Bethe lattices of connectivities $k+1=3\ldots,26$ at $T=0$ are approximated numerically. To obtain sufficient accuracy for large system sizes (up to $n=2^{12}$), the Extremal Optimization heuristic is employed which provides high-quality results not only for the ground state energies per spin e_{k+1} but also for their entropies s_{k+1}. The results indicate sizable differences between lattices of even and odd connectivities. The extrapolated ground state energies compare very well with recent one-step replica symmetry breaking calculations. These energies can be scaled for all *even* connectivities $k+1$ to within a fraction of a percent onto a simple functional form, $e_{k+1}=E_{SK}\sqrt{k+1}-(2E_{SK}+\sqrt{2})/\sqrt{k+1}$, where $E_{SK}=-0.7633$ is the ground state energy for the broken replica symmetry in the Sherrington-Kirkpatrick model. But this form is in conflict with perturbative calculations at large $k+1$, which do not distinguish between even and odd connectivities. We also find non-zero entropies per spin s_{k+1} at small connectivities. While s_{k+1} seems to vanish asymptotically with $1/(k+1)$ for even connectivities, it is numerically indistinguishable from zero already for odd $k+1\geq 9$.

PACS. 75.10.Nr Spin-glass and other random models – 02.60.Pn Numerical optimization – 89.75.-k Complex systems 05.10.-a Computational methods in statistical physics and nonlinear dynamics

1 Introduction

In this paper we study the ground state ($T=0$) properties of $\pm J$ spin glasses on $k+1$-Bethe lattices [1]. The Bethe lattices in this case are r-regular graphs [2] with $r=k+1$. These are randomly connected graphs consisting of n vertices in which each vertex has a fixed connectivity of $k+1$. This constraint contrasts with "random graphs" [2,3] in which pairs of vertices are randomly connected, leading to a Poissonian distribution of connectivities around a mean of $\langle c\rangle$; these graphs will be studied numerically elsewhere [4]. We explore the large-n regime of low-connectivity graphs, $k+1=3,\ldots,26$, which are of great theoretical interest as finite-connected, mean-field models for low-dimensional lattice spin glasses [5,6]. A great number of studies have focused on various aspects of this conceptually simple model to hone the complex mathematical techniques required to treat disordered systems [1,7–12] or optimization problems [14–19]. In this paper we will try to provide a independent numerical check on the validity and accuracy of those techniques.

Our results, in turn, reflect on the flexibility of the extremal optimization (EO) heuristic [20,21] in finding approximate but high-quality solutions for ground states of spin glasses on an arbitrary graphical structure in a reasonable computational time. These are often NP-hard optimization problems which are believed to require a computational effort that rises faster than any power of n to obtain provably exact solutions [22]. Thus, exact methods as of yet are not able to provide results for large-n problems, at least not with significant statistics [23], except for some special cases [24–26]. Furthermore, there is only a small number of capable approximate algorithms available for the study of $T=0$ properties of spin glasses [27–29], mostly restricted to d-dimensional lattice models, and EO provides a distinct alternative which will increase the confidence in the numerical results available. In previous papers, we have demonstrated the capabilities of EO in determining near-optimal solutions by reproducing existing results for $3d$ and $4d$ spin glasses and obtaining new results for the coloring problem [21,30] and the graph partitioning problem [20,31,32]. The results in this paper show that EO is not only capable of approximating ground states well but also of sweeping the entire configuration space efficiently to determine the degeneracy of ground states [30]. Unlike other methods, EO never "freezes" into local minima and proves to be limited mostly by the inability to store new ground states.

We find that our results for the ground state energies are consistent with the theoretical results of the assumption of replica symmetry-breaking (RSB) in the $\pm J$ spin glass on $k+1$-connected Bethe lattices. Our numerical result for $k+1=3$ below clearly excludes the replica

[a] e-mail: stb@physics.emory.edu
www.physics.emory.edu/faculty/boettcher

symmetric (RS) solution and are within 0.1% of the one-step replica symmetry-broken (1RSB) result [1]. While 1RSB is by far not a full RSB solution, the numerical result corroborates the expectation that higher order corrections would be small. Beyond that our results suggest subtle differences between even and odd values of the connectivity $k+1$, with no obvious way to continue smoothly between them [33]. These oscillations may doom perturbative calculation for $k+1 \to \infty$ [8,11]. We find that the entropy is finite and decaying like $1/(k+1)$ for large, even $k+1$. For odd $k+1$ it is non-zero only for small values and may be vanishing already beyond some finite, odd connectivity.

In the following we introduce first the Bethe lattices we used in the numerical calculations. In Section 3 we briefly describe the EO algorithm which is amply discussed elsewhere [20,21,34]. In Section 4 we present a few simulations to reproduce known results to gauge our procedure. In Section 5 we present our numerical results, including an extensive discussion in Section 5.3. Some conclusions are presented in Section 6.

2 Spin glasses on Bethe lattices

Disordered spin systems on random graphs have been investigated as mean-field models for low-dimensional spin glasses or optimization problems, since variables are long-range connected yet have a small number of neighbors. Particularly simple are Bethe lattices of connectivity $k+1$ [1,7,9], also called fixed-valence or r-regular random graphs [2,19,31,35]. These are graphs consisting of n vertices where each vertex possesses a fixed number $k+1$ of bonds with randomly selected other vertices. In comparison to the otherwise more familiar random graphs studied by Erdös and Rény [2,3], Bethe lattices at a given n and k avoid fluctuations in the connectivities of vertices and in the total number of bonds.

There are slight variations in the generation of Bethe lattices. For instance, to add a bond one could choose at random two vertices of connectivities $< k+1$ to link until all vertices are $k+1$-connected. Instead, we have used the method described in reference [2] to generate these graphs. Here, all the terminals on the vertices form a list of $n(k+1)$ independent variables. For each added bond two available terminals are chosen at random to be linked and removed from the list. Furthermore, for algorithmic convenience, we reject graphs which possess self loops, bonds that connect two terminals of the same vertex. Multiple bonds between any pair of vertices are allowed, otherwise it is too hard to generate feasible graphs for, say, $n = 32$ and $k+1 = 20$. Since $k+1$ remains finite for $n \to \infty$, the energy and entropy per spin would only be effected to $O(1/n)$ by the differences between these choices.

Once a graphical instance is generated, we assign randomly chosen but fixed couplings $J_{i,j} \in \{-1, +1\}$ to existing bonds between neighboring vertices i and j. Each vertex i is occupied by a spin variable $x_i \in \{-1, +1\}$. The energy of the system is defined as the difference in number between violated bonds and satisfied bonds,

$$H = -\sum_{\{bonds\}} J_{i,j} x_i x_j, \tag{1}$$

and in this paper we will focus on the energy per spin,

$$e_{k+1}(n) = \frac{1}{n}\langle H \rangle, \tag{2}$$

as a function of $k+1$ in the limit of $n \to \infty$. Averages are taken over all randomly generated instances of graphs and of bond assignments. Each instance can have a large degeneracy Ω in the configurations exhibiting its ground state energy, and we also sample their average entropy per spin,

$$s_{k+1}(n) = \frac{1}{n}\langle \ln \Omega \rangle. \tag{3}$$

3 τ-EO algorithm for Bethe lattices

The extremal optimization algorithm, τ-EO, which we employ in this paper, has been discussed previously in [21], and in [32,35] with regard to the setting of its one free parameter, τ. Here, we merely describe the implementation of τ-EO without further justification.

To obtain the numerical results in Sections 4–5, we used the following implementation of τ-EO: For a given spin configuration on a graph, assign to each spin x_i a "fitness"

$$\lambda_i = -\#\text{violated bonds} = 0, -1, -2, \ldots, -(k+1), \tag{4}$$

so that

$$e_{k+1} = -\frac{1}{n}\sum_i \lambda_i - \frac{k+1}{2} \tag{5}$$

is satisfied. Each spin falls into one of only $k+2$ possible states. Say, currently there are n_{k+1} spins with the worst fitness, $\lambda = -(k+1)$, n_k with $\lambda = -k$, and so on up to n_0 spins with the best fitness $\lambda = 0$. Now draw a "rank" l according to the distribution

$$P(l) = \frac{\tau - 1}{1 - n^{1-\tau}} l^{-\tau} \quad (1 \le l \le n). \tag{6}$$

Then, determine $0 \le j \le (k+1)$ such that $\sum_{i=j+1}^{k+1} n_i < l \le \sum_{i=j}^{k+1} n_i$. Finally, select any one of the n_j spins in state j and reverse its orientation *unconditionally.* As a result, it and its neighboring spins change their fitness. After all the effected λ's and n's are reevaluated, a new spin is chosen for an update.

This EO implementation updates spins with a (τ-dependent) bias against poorly adapted spins on behalf of equation (6). This process is "extremal" in the sense that it focuses on atypical variables, and it forms the basis of the EO method. The only adjustable parameter in this algorithm is the power-law exponent τ. For $\tau = 0$,

randomly selected spins get forced to update, resulting in a random walk through the configuration space which would yield poor results. For $\tau \to \infty$, only spins in the worst state get updated which quickly traps the update process to a small region of the configuration space which may be far from a near-optimal solution. The arguments given in [35] and a few experiments indicate that $\tau = 1.3$ is a good choice to find ground states efficiently on Bethe lattices.

The algorithm never converges or "freezes" into a particular state but perpetually explores new near-optimal configurations. It is, of course, easy to simply store the lowest energy state found so far in a given run of τ-EO and terminate when desired. Previous experience with optimizing spin glasses with EO [21], and a few experiments, suggest a typical number of updates of $O(n^3)$ for an EO-run to obtain saturation in the values found for ground states, at least up to the system sizes $n \approx 10^3$ obtainable here. Instead of pushing to attain larger values of n, we opt here for obtaining better statistics by sampling more instances at smaller values of n while spending even more time on each instance than may seem to be required, in an attempt to ensure accuracy. In particular, our implementation restarts for each instance at least $r_{\max} = 4$ times with new random initial spin-assignments, executing $\approx 0.1\, n^3$ updates per run. If a new, lower-than-previous energy state is encountered in run r, we adjust $r_{\max} = 2 + 2r$ for that instance so that EO runs at least *twice* as many restarts as were necessary to find the lowest state in the first place. Especially for small n, $r_{\max}$ hardly ever exceeds 4; for larger n a few graphs require up to 25 restarts before termination.

Since EO perpetually explores new configurations it is well suited to explore also the degeneracy of low-energy states. In this case we not only store the first configuration found with the lowest energy for that instance. Instead, we consider each configuration with the lowest energy, retaining new ones and rejecting all others. This procedure is somewhat inefficient and at best allows system sizes up to $n = 256$ beyond which the degeneracy exceeds memory constraints. But it provides a fast way to also determine the $T = 0$ entropy of the ground states with moderate accuracy. In these runs, we used a similar approach to the above, except for setting $r_{\max} = 8 + 2r$ where r is the latest run in which another new configuration of the lowest energy was located. Here, for some highly degenerate instances at larger n, $r_{\max}$ could reach up into the 100's, further limiting attainable system sizes.

4 Numerical test

To evaluate the proposed τ-EO algorithm, we have run a series of test. First, we can defer to some already published results [21,35]. In reference [21] we have calculate approximations to the ground state energy for $\pm J$ spin glasses on a hyper-cubic lattice for $d = 3$ and $d = 4$ for systems up to $n = 12^3 = 1728$ which for each n reproduced previous results obtained with sophisticated genetic algorithms [27,28] (although there we used a fixed $r_{\max}$). To evaluate the ability of the algorithm to determine the degeneracy of low-energy states found, we have reproduced within statistical error the results of reference [36] up to $n = 6^3$ beyond which EO ran out of time and memory to sample states completely. (Ref. [36] used a more efficient way to estimate the entropy from sampling only a small number of states.) And it took EO only a fraction of a second to find all 60 ground states of a 4^3 instance that had been exactly enumerated in reference [23].

To gauge τ-EO's performance for larger n, we have run our implementation also on two $3d$ lattice instances, *toruspm*3-8-50 and *toruspm*3-15-50, with $n = 8^3 = 512$ and $n = 15^3 = 3375$, considered in the 7th DIMACS challenge for semi-definite problems [37]. Bounds [38] on the ground-state cost established for the larger instance are $H_{\rm lower} = -6138.02$ (from semi-definite programming) and $H_{\rm upper} = -5831$ (from branch-and-cut). EO found $H_{\rm EO} = -6049$ (or $H/n = -1.7923$), a significant improvement on the upper bound and already lower than $\lim_{n\to\infty} H/n \approx 1.786\ldots$ found in references [21,27,28]. Furthermore, we collected 10^5 such states, which roughly segregate into 3 clusters with a mutual Hamming distance of at least 100 distinct spins; at best a small sample of the $\approx 10^{73}$ ground states expected [36]! For the smaller instance the bounds given are -922 and -912, resp., while EO finds -916 (or $H/n = -1.7891$) and was terminated after finding 10^5 such states. While this run (including sampling degenerate states) took only a few minutes of CPU (at 800 MHz), the results for the larger instance required about 16 hours.

Finally, we note that we have considered the algorithm for making Bethe lattices previously in references [31,35]. In reference [31] we have studied the graph bi-partitioning problem and found that the ground state energy was well above previous RS calculations from reference [9], but only minutely below numerical calculations obtained using simulated annealing [19]. In reference [35] we have considered some variations in the generation of Bethe lattices and found that they effect the results only in next-to-leading order.

5 Numerical results for Bethe lattices

We have simulated Bethe lattices with the algorithm described in Section 3 for $k + 1$ between 3 and 26, and graph sizes $n = 2^l$ for $l = 5, 6, \ldots, 12$ to obtain results for ground state energies, and for $n \in [16 \ldots 256]$ to determine their entropy. In the following, we present the results for ground-state energies and entropies from those simulations. The results are discussed in detail in Section 5.3.

5.1 Ground state energies

To reach relative statistical errors of our averages roughly uniform with n we generated initially a number of $10^5/\sqrt{n}$ instances for each n and $k + 1$. Fortunately, deviations appear to narrow much faster than $1/\sqrt{n}$, and thus we

Table 1. Data from the EO simulations for the average ground-state energy per spin $e_{k+1}(n)$, plotted also in Figures 1 and 2.

n	$-e_3(n)$	$-e_4(n)$	$-e_5(n)$	$-e_6(n)$	$-e_7(n)$	$-e_8(n)$	$-e_9(n)$	$-e_{10}(n)$	$-e_{15}(n)$	$-e_{20}(n)$	$-e_{25}(n)$
32	1.195(1)	1.3506(6)	1.5543(6)	1.6734(8)	1.8424(8)	1.9425(9)	2.0906(9)	2.1730(33)	2.7013(40)	3.1056(48)	3.4923(51)
64	1.2231(3)	1.3964(4)	1.5979(4)	1.7294(5)	1.8972(5)	2.0083(6)	2.1551(6)	2.2557(23)	2.7884(28)	3.2090(33)	3.6029(37)
128	1.2426(5)	1.4245(10)	1.6269(10)	1.7652(12)	1.9335(13)	2.0476(14)	2.1945(15)	2.3042(16)	2.8443(20)	3.2742(23)	3.6731(25)
256	1.2542(3)	1.4417(6)	1.6434(7)	1.7885(8)	1.9549(8)	2.0782(10)	2.2204(10)	2.3324(11)	2.8774(14)	3.3186(16)	3.7215(18)
512	1.2608(2)	1.4534(4)	1.6548(5)	1.8020(5)	1.9685(6)	2.0934(6)	2.2379(7)	2.3488(7)	2.8993(10)	3.3435(11)	3.7505(12)
1024	1.2644(1)	1.4603(3)	1.6612(3)	1.8110(3)	1.9762(5)	2.1035(5)	2.2470(5)	2.3605(5)	2.9092(7)	3.3551(9)	3.7612(11)
2048	1.2673(1)										
4096	1.2689(2)										
∞	1.2716(1)	1.472(1)	1.673(1)	1.826(1)	1.990(3)	2.121(1)	2.2645(5)	2.378(3)	2.935(1)	3.389(1)	3.806(4)

Table 2. Some properties of the numerical computations. Listed are for each n the number of instance used and the average number of updates for each instance needed to obtain the results listed in Table 1.

n	Instances	t
32	19444	3.0×10^2
64	13750	1.5×10^3
128	883	1.0×10^4
256	625	1.6×10^5
512	441	3.1×10^6
1024	312	7.6×10^7
2048	220	1.5×10^8
4096	25	2.4×10^9

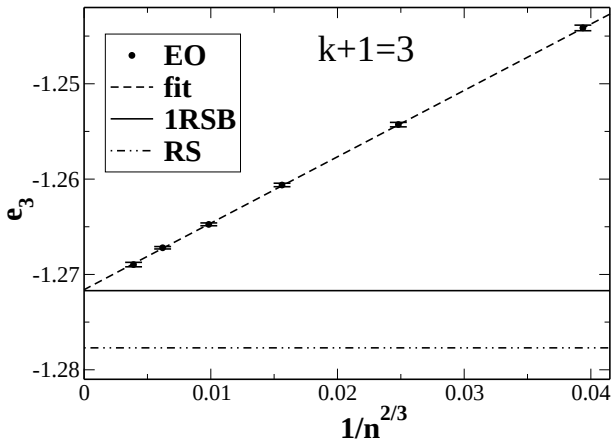

Fig. 1. Extrapolation plot for the EO data for $k+1 = 3$ given in Table 1 and the fitted curve according to equation (7). For $n \to \infty$ the extrapolation gives $e_3 = -1.2716(1)$, way above the RS result but consistent with the 1RSB result from reference [1], both indicated by horizontal lines.

added more instances at smaller n with small extra computational cost to obtain narrow error bars there as well. In Table 1 we list the values of average energies according to equation (2), $e_{k+1}(n)$, for each $k+1$ and n. The number of instances used and the average number of update steps required are listed in Table 2. The results for the number of updates has been also averaged over all connectivities $k+1$, although lower-connected graphs require typically fewer updates. Note that this is the *minimal* number of updates needed to obtain the listed results, the actual number of updates taken up by each run of EO to ensure convergence was at least twice of that but could be much larger, according to the specification of the algorithm in Section 3.

Unfortunately, when plotted as a function of $1/n$, the average energies for each given $k+1$ clearly do not extrapolate linearly (as, for example, seems to be the case for spin glasses on a hyper-cubic lattice [21,27,28]). Instead, using an extrapolation according to [1]

$$e_{k+1}(n) \sim e_{k+1} + \frac{A}{n^\nu} \quad (n \to \infty). \tag{7}$$

[1] In a previous simulation [35], we have attempted to fit a smaller set of data (at $k = 1 = 3, 4$) with a $\ln(n)/n$ correction with a result that was somewhat above the current extrapolation value.

We find that for the whole range of connectivities $k+1$ studied here, the scaling corrections appeared to be consistent with $\nu = 2/3$ within a few percent, except for two outliers at $k+1 = 10$ and 25. Thus, we have plotted for each $k+1$ the values of $e_{k+1}(n)$ as a function of $1/n^{2/3}$ in Figures 1 and 2. Although the extrapolation appears to be linear on that scale for each $k+1$, we have fitted the data with the more general form of equation (7). (Fits were weighted according to n and to the inverse of the standard deviation for each point.) These fits are also shown as dashed lines in each of the Figures 1 and 2.

The extrapolation results for the ground state energies appear to be quite stable under variation of the scaling form, for instance, when fitting with fixed $\nu = 2/3$ instead of equation (7). We estimate that each has a relative error of about $< 0.3\%$. Exceptions to this estimate we have to grant for the cases of $k+1 = 10$ and 25, in which case we also observe significant differences to the $\nu = 2/3$ corrections to scaling. Throughout, the extrapolated energies are consistent with recently given lower bounds [39].

We can compare our results with existing theoretical predictions at the RS and the 1RSB level at least for

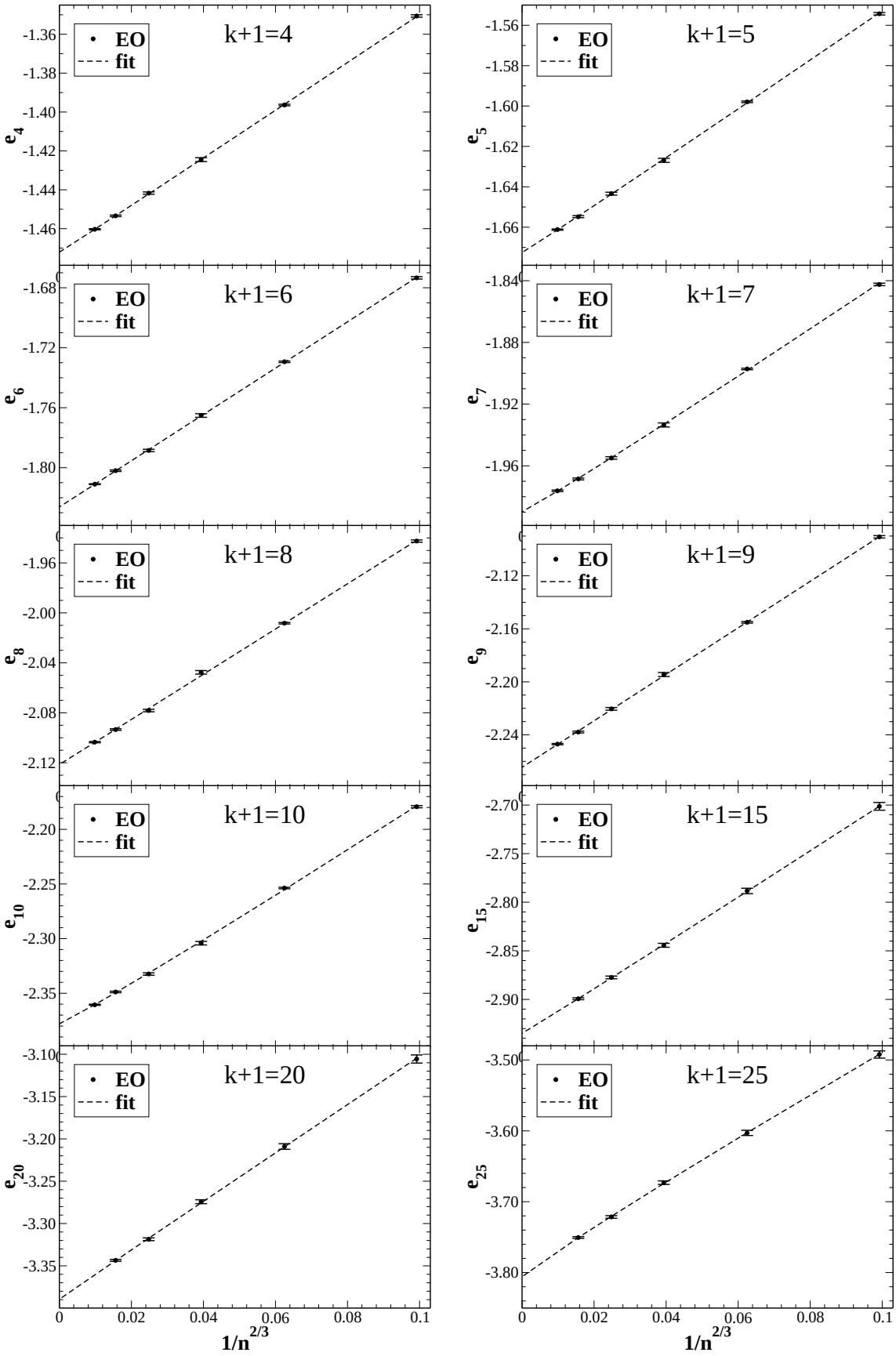

Fig. 2. Extrapolation plot for the EO data in Table 1 for $k+1=4$ to 25, as in Figure 1. All data seems to extrapolate well linearly in $1/n^{2/3}$. The extrapolated values of e_{k+1} for $n \to \infty$ are also listed in Table 1.

the case of $k+1=3$. For this case, a recently published calculation [1] yielded $e_3 = -1.2777$ at the RS, and $e_3 = -1.2717$ at the 1RSB level. These values are also indicated in Figure 1. Clearly, our result for $k+1$ is consistent with the 1RSB results, but certainly inconsistent with the RS result. The numerical result corroborates the claim from reference [1] that corrections from the full RSB solution would be small. Further 1RSB results for other values $k+1$ are currently being calculated [40]. We will present a more detailed analysis of the extrapolated values of e_{k+1} at $n \to \infty$ in Section 5.3.

5.2 Ground state entropy

We have also used EO to sample the degeneracy Ω of the lowest-energy states found. Due to the discrete nature of the energy of the system, ground-states can be highly degenerate, and the ground-state entropy per spin defined in equation (3) may well be non-vanishing for $n \to \infty$. While the search for a ground state of an instance is certain to provide a rigorous upper bound to the actual ground state energy, the search for the complete set of ground states for an instance entails the risk of two competing systematic errors: (1) If EO misses to find the exact ground state, one is likely to vastly over-count the degeneracy, since Ω is expected to rise exponentially with the energy above the ground state [41]. (2) Even if EO finds ground states, it may simply undercount Ω, since such states could be too far separated in configuration space. Therefore, we have implemented EO with the settings described in Section 3, which emphasize the desire for accuracy over computational efficiency. Accordingly, we were bound to conduct a separate set of simulations from those that determined the energies only. In these simulations we focused on smaller system sizes of $n \leq 256$ for $k+1 = 3, \ldots, 9$ and $10, 14, \ldots, 26$ only. The limit on n for the smaller $k+1$ is mostly dictated by avoiding system sizes at which Ω typically exceeds 10^6.

As a test for the accuracy of our implementation, we have run the simulation for $k+1=3$ twice on the exactly identical instances, using different initial conditions and $n/5$ more updates in the second run: The results, both for the energies and Ω, were identical *for each instance,* producing the same set of configurations independent of the starting point of the search. We therefore assume that systematic errors in our data are small and can be neglected.

Since the range of system sizes n is smaller than for the case of the energies, it is more difficult to extrapolate our data for $s_{k+1}(n)$. Again, it is clear that the corrections are not linear in $1/n$, but instead seems to be scaling close to $1/n^{2/3}$ for all $k+1$, as for the energies above. Considering the limitations on n, we assume that the corrections are exactly of that form and extrapolate our data simply with a fit to

$$s_{k+1}(n) \sim s_{k+1} + \frac{A}{n^{2/3}} \quad (n \to \infty), \tag{8}$$

again, weighting each data point with respect to n and the inverse of its error. As the systematic and statistical uncertainties of our data appears to be small, the uncertainty about the scaling corrections must be considered the most significant limitation on accuracy in our extrapolation. The data and the extrapolation fits according to equation (8) are shown in Figures 3 and 4. The results for s_{k+1} for $n \to \infty$ are listed in Table 3.

The data clearly shows a different quantitative behavior between odd and even values of $k+1$. This difference for the entropies can be explained in terms of the "free spins:" In a highly frustrated system, even near ground states, many spins are stuck in a situation in which they violate many of their constraints, no matter how they are oriented, and changing from one direction to the other may hardly change the energy of the system. In particular, an even-connected spin that happens to violate exactly half of its bonds (with $J = \pm 1$) can flip freely without any change to the energy. Odd-connected spins can only become "free" in a connected pair (that happens to violate exactly half of its *external* bonds but satisfies their mutual bond) in which both simultaneously flip without changing the energy. The latter situation is naturally far less likely, and thus, purely even-connected graphs exhibit far more potential for degeneracy at the ground state than the corresponding odd-connected graphs. Some preliminary studies for $k+1 = 3$ and 4 show that in ground state configurations the fraction of free spins (zero by design for $k+1=3$) converges to a value just around 5% for $k+1=4$, while the fraction of free pairs seems to vanish for large n for both, even and odd $k+1$. We have not explored the clustering of these states [36]. We will explore the different behaviors for even and odd $k+1$ in the next section.

5.3 Discussion of the extrapolation results

In this section, we want to focus on some of the curious properties exhibited by the values of the energies and entropies found by extrapolation in the previous section. We have already noted the difference between the entropies for even and odd values of $k+1$. Such behavior for these Bethe lattices has been observed previously [39]. In fact, there are similar differences, although more subtle, for the energies e_{k+1}. These differences become most apparent when we plot the data asymptotically for large $k+1$, where it is known that

$$\lim_{k+1\to\infty} \frac{e_{k+1}}{\sqrt{k+1}} = E_{SK}, \tag{9}$$

with $E_{SK} = 0.7633$ being the RSB ground state energy of the Sherrington-Kirkpatrick model [6,42]. In Figure 5 we have plotted $e_{k+1}/\sqrt{k+1}$ as a function of $1/(k+1)$. On this scale, we notice that the energies split into a set of even and a set of odd values [2], each located apparently on a straight line. Even though $k+1 \leq 25$ is quite small, each line separately extrapolates very close to the exact value for large $k+1$ indeed: $E_{SK}^{even} \approx -0.763$ and $E_{SK}^{odd} \approx -0.765$.

[2] Curiously, the oscillations in the energy bounds observed by reference [39] are exactly out of phase with this data.

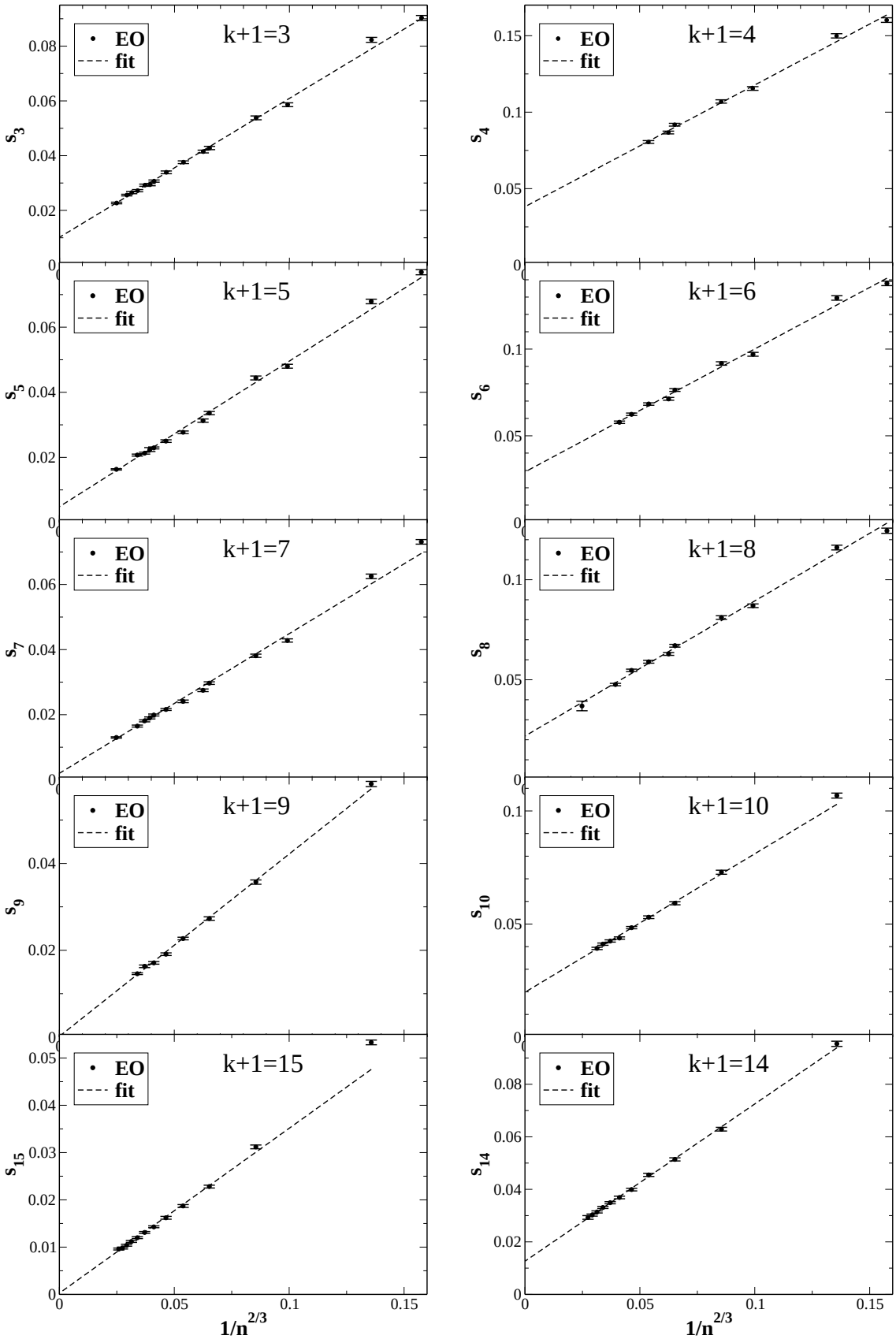

Fig. 3. Extrapolation plot for the EO data for the entropy $s_{k+1}(n)$ for $k+1 = 3$ to 15. All data seems to extrapolate well linearly in $1/n^{2/3}$. Note the difference in the results between odd (left) and even (right) $k+1$. The extrapolated values of s_{k+1} for $n \to \infty$ are listed in Table 3.

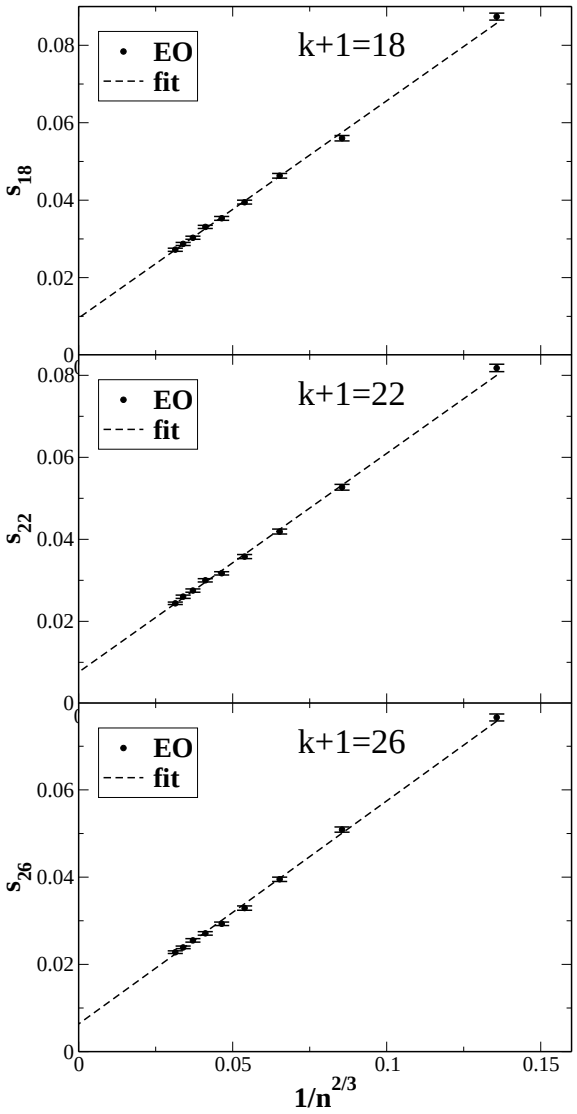

Fig. 4. Extrapolation plot for the EO data for the entropy $s_{k+1}(n)$ for some larger, even $k+1$, similar to Figure 3.

Even more amazing, the value of $e_2 = -1$ (see Eq. (16) below) for the trivial $k+1 = 2$ Bethe lattice is very close to the linear fit for the even EO results. Clearly, a function that would interpolate continuously *all* the data will have to be very complicated (oscillatory). But could it be that its envelope on the even and the odd integers happens to be simple? Then, in case of the even data [3], we could even write down the exact form of the function for $\mathcal{E}_{k+1}$ that would fit the data, since it has to pass $e_2 = -1$ and satisfy equation (9), to wit:

$$\mathcal{E}_{k+1} = \sqrt{k+1}E_{SK} - \frac{2E_{SK} + \sqrt{2}}{\sqrt{k+1}}. \qquad (10)$$

To test equation (10), we plot the data in Figure 6 as $e_{k+1}/\mathcal{E}_{k+1}$ to study its deviations from the conjecture.

[3] Although the odd data may equally well be fitted in this way, the line can not be determined since only one point on it, E_{SK}, is exactly known.

Table 3. Extrapolation results for the entropies per spin for the data plotted in Figures 3 and 4.

$k+1$	s_{k+1}	$k+1$	s_{k+1}
3	0.0102(10)	4	0.0381(15)
5	0.0048(10)	6	0.0291(10)
7	0.0020(10)	8	0.0218(10)
9	0.0002(15)	10	0.0198(10)
15	0.0002(15)	14	0.0126(10)
		18	0.0095(10)
		22	0.0076(10)
		26	0.0063(15)

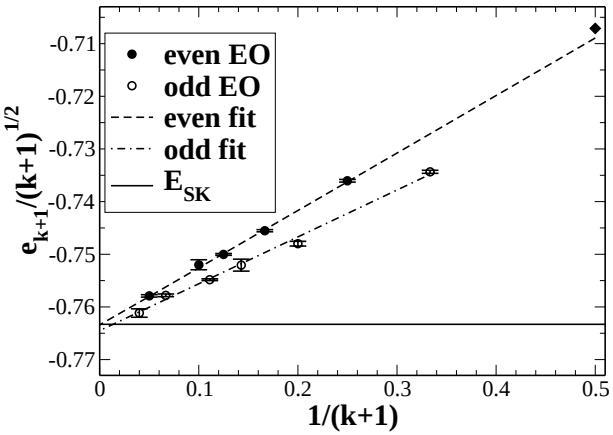

Fig. 5. Plot of the rescaled extrapolated energies, $e_{k+1}/\sqrt{k+1}$, as a function of $1/(k+1)$. The data appears to fall on two separate straight lines for even and for odd $k+1$. The straight line provides an excellent fit all the way from the exact result $e_2 = -1$ (diamond) to $E_{SK} = -0.7633$ (horizontal line) at $k+1 \to \infty$.

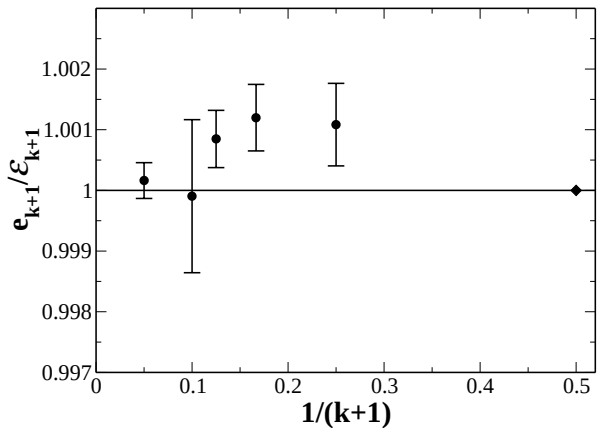

Fig. 6. Plot of the energies relative to the conjectured function $\mathcal{E}_{k+1}$ in equation (10) as a function of $1/(k+1)$. All data for even $k+1$ falls within about 0.1% of $\mathcal{E}_{k+1}$ (*i.e.* the horizontal line). The point at $k+1 = 2$ (diamond) is exact by definition, of course.

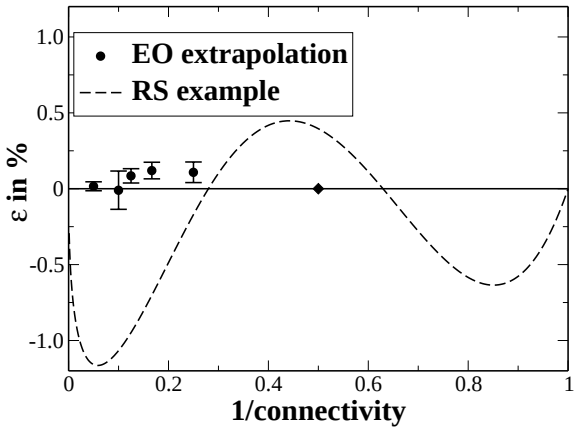

Fig. 7. Plot of the relative error ϵ in % between the extrapolated data and the function in equation (10), as before in Figure 6, but now superimposed with the corresponding result obtained for the exactly solvable RS spin glass on random graphs [43]. Note the order-of-magnitude larger deviations from the reference line for the RS example.

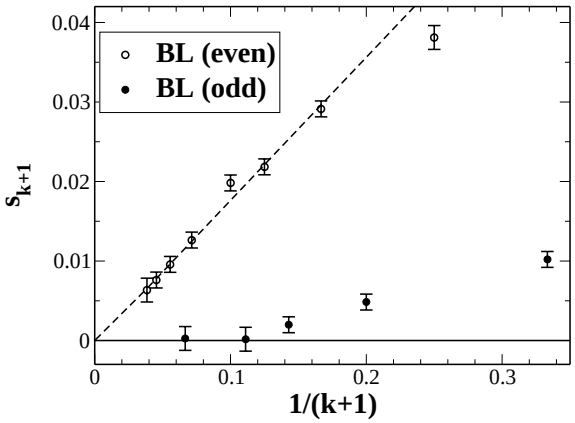

Fig. 8. Asymptotic plot of the extrapolated entropies from Table 3 as a function of $1/(k+1)$. The data for even $k+1$ seems to vanish linearly with $1/(k+1)$ (dashed line). The data for odd $k+1$ drops more precipitously, and can not reasonably be fitted at this level of accuracy.

While the extrapolated values do not fall exactly within their (estimated) error bars on the proposed form, they are indeed within about 0.1% of it. To judge how close the data is to the proposed functional form in equation (10), we utilize a closely related example. The ground-state energy as a function of the (continuous) average connectivity $\langle c\rangle$ is known exactly for the RS case of ordinary random graphs with fluctuating internal connectivities, equation (16) in reference [43]. If one plots that solution (which involves exponentials and modified Bessel functions) in the same way as e_{k+1} in Figure 5, one notes that it, too, could be approximated surprisingly well with a straight line, $-\sqrt{2c/\pi}+(\sqrt{2/\pi}-\frac{1}{2})/\sqrt{c}$, now crossing the RS ground state energy $-\sqrt{2/\pi}$ [6] for $\langle c\rangle\to\infty$ and reaching the trivial result of $-1/2$ at the percolation point $\langle c\rangle=1$. In Figure 7 we superimpose the relative error of this approximation with respect to the exact RS result, with the relative error of our data with respect to the conjecture. It shows that the error of the conjecture is still almost by an order of magnitude smaller than the global bound for the RS test case, thus putting a significant bound on any corrections similar in type to equation (16) in reference [43].

The differences between even and odd connectivities are even more pronounced in case of the entropies, as we have explained in Section 5.2. Thus, although our data for the entropy is not nearly as accurate as for the energies, it is still instructive to study it in more detail. In Figure 8, we plot the extrapolated values of the entropies from Table 3 to explore its decrease for large $k+1$. Despite the large error bars, a significant *qualitative* difference between even and odd data points is visible: The entropy for even values of $k+1$ decays slowly, apparently linearly with $1/(k+1)$. On the other hand, the entropies for odd $k+1$ drop much more rapidly, and are already indistinguishable from zero (within our errors) for $k+1=9$, while it is clearly non-vanishing for $k+1=3$ (unless our assumption about the scaling corrections in equation (8) are incredibly wrong (see Fig. 3)). Unfortunately, with only a small, discrete number of data points available that are significantly above zero, it is very hard to decide whether the entropy for odd $k+1$ merely decays too rapidly, or whether there exists a finite value of $k+1$ above which all odd entropies become identically zero.

6 Conclusion

In this paper we have presented an extensive numerical study of the ground states of spin glasses on Bethe lattices. The available data possess sufficient accuracy to obtain extrapolated values for ground state energies and entropies at the 0.1% and the 10% level, respectively. In both cases, significant differences emerge between the data for odd and even values of $k+1$. Based on the numerical results, we have shown that the extrapolated energies for *all* even values of $2\le k+1\le\infty$ are well fitted with a simple function, equation (10). Furthermore, the data suggests that the entropies per spin are generally non-zero at small $k+1$, but may vanish above a finite $k+1$ for odd values.

Of course, there is plenty of reason to doubt that such a simple result as equation (10), albeit confined to discrete integer values of $k+1$, could indeed be the solution to a complex RSB problem. In fact, one argument against the conjecture is a discrepancy in its prediction for large $k+1$ at next-to-leading order. Several authors [8,12] have studied spin glasses on random graphs beyond the RS level perturbatively for $k+1=z\to\infty$ to determine the $1/z$ correction f_1 to the free energy (at $T>0$) in $E_{SK}+f_1/z$. Interpreting the results recently presented in reference [8], the correction for fixed connectivities for $T\to 0$ would be about $f_1=-0.317$, while equation (10) would predict about 0.1124. It should be noted, though, that the $1/z$ expansion implicitly assumes a smooth continuation off the integers which may lead to ambiguities in light of the oscillatory behavior between even and odd integers we found

for the ground states in Figure 5 (similar to the continuation of, say, the function $\cos(2\pi z)/z$ for $z \to \infty$).

In any case, future calculations like the one in reference [1] but for even $k+1$ will provide a check on both, our extrapolated data and the conjecture.

This work has been supported under a grant from the Emory University Research Committee. I am greatly indebted to Marc Mézard for his helpful comments.

Appendix

The case $k+1=2$

Clearly, a Bethe lattice in which each vertex has exactly 2 connections can only consists of a collection of disconnected loop graphs. We merely need to determine the number of loops and their size distribution to derive the average ground state energy and entropy. Each loop has a 50% chance of being frustrated, thus, the number of cut bonds is equal to one-half of the number of loops, and the degeneracy is equal to the length of these loops to the power of their number.

To analyze the $k+1=2$ case we consider each of the n vertices as a node with two terminals. Adding lines can create two types of objects: strings and loops. We consider, after adding t lines, an individual vertex as a string of length 0, of which there are $l_{0,t}$; in general, we have $l_{i,t}$ strings of length i, each possessing two open terminals. In particular, before we added any lines: $l_{i,t=0} = n\delta_{i,0}$. A loop of length i is created by addition of a line to both open terminals of a string of length $i-1$. There are $p_{i,t}$ loops of length i after adding t lines which can not evolve further, since they don't possess any more open terminals. We start with $2n$ open terminals and cover 2 of those with each newly added line. We can identify two constraints:

$$\sum_{i=0}^{\infty} l_{i,t} = n - t, \qquad \sum_{i=1}^{\infty} i\,(l_{i,t} + p_{i,t}) = t. \tag{11}$$

After adding t lines at random, there are $2(n-t)$ terminals left to accommodate the next line, allowing for $\binom{2(n-t)}{2}$ different choices. Accounting for all possible choices, we obtain

$$\begin{aligned} l_{0,t+1} &= \left[1 - \frac{2}{n-t} + \frac{1}{\binom{2(n-t)}{2}}\right] l_{0,t}, \\ l_{i,t+1} &= \left[1 - \frac{2}{n-t} + \frac{1}{\binom{2(n-t)}{2}}\right] l_{i,t} \\ &\quad + \frac{2}{\binom{2(n-t)}{2}} \left(\sum_{j=0}^{i-1} l_{j,t} l_{i-1-j,t} - l_{\frac{i-1}{2},t}\big|_{i\,\mathrm{odd}}\right), \\ p_{i,t+1} &= p_{i,t} + \frac{1}{\binom{2(n-t)}{2}} l_{i-1,t}, \end{aligned} \tag{12}$$

where $i > 0$. It is easy to show that these equations satisfy the constraints in equations (11).

We can transform these equations by defining $\theta = t/n$, $\mathrm{d}\theta = 1/n$, $y(x,\theta) = \frac{1}{n}\sum_{i=0}^{\infty} l_{i,t} x^i$, and $p(x,\theta) = \sum_{i=0}^{\infty} p_{i,t} x^i$. Considering n large and θ continuous, equations (12) turn into

$$\begin{aligned} \frac{\mathrm{d}y(x,\theta)}{\mathrm{d}\theta} &= -\frac{2y(x,\theta)}{1-\theta} + \frac{x[y(x,\theta)]^2}{(1-\theta)[1-\theta-1/(2n)]} \\ &\quad + \frac{1}{n}\left[\frac{y(x,\theta) - xy(x^2,\theta)}{2(1-\theta)[1-\theta-1/(2n)]}\right], \\ \frac{\mathrm{d}p(x,\theta)}{\mathrm{d}\theta} &= \frac{xy(x,\theta)}{(1-\theta)^2}, \\ y(x,0) &= 1, \qquad p(x,0) = 0. \end{aligned} \tag{13}$$

Luckily, for $n \to \infty$, the equations are easily solved to give

$$y(x,\theta) = \frac{(1-\theta)^2}{1-x\theta}, \qquad p(x,\theta) = -\frac{1}{2}\ln(1-x\theta). \tag{14}$$

Finally, the total number of loops for the (almost) completed graph, $\theta = 1 - 1/n$, is given by

$$p(1, 1-1/n) = \sum_{i=1}^{\infty} p_{i,n-1} \sim \frac{1}{2}\ln(n). \tag{15}$$

On average, half of these loops will be frustrated, *i.e.*, they will have one of their bonds violated. Since the Hamiltonian in equation (1) counts the difference between violated and satisfied bonds, or twice the violated bonds minus the number of all bonds, $n(k+1)/2 = n$, we get

$$e = \frac{1}{n}\langle H\rangle \sim -1 + \frac{\ln(n)}{2n}\cdot \tag{16}$$

Similarly, we can estimate the degeneracy Ω of these ground states, roughly, as the average length of loops, $\langle i\rangle = \partial_x \ln p(x, 1-1/n)|_{x=1} \sim n/\ln(n)$, taken to the power of one-half of their number, $\ln(n)/(4n)$, to give

$$s = \frac{1}{n}\ln\Omega \sim \frac{\ln(n)^2}{4n}\cdot \tag{17}$$

(The logarithmic corrections in this result may not be exact.) Clearly, both the number of violated bonds as well as the entropy per spin vanish in the large-n limit.

References

1. M. Mézard, G. Parisi, *Cavity method at zero temperature*, `cond-mat/0207121`
2. B. Bollobas, *Random Graphs* (Academic Press, London, 1985)
3. P. Erdös, A. Rényi, in *The Art of Counting*, edited by J. Spencer (MIT, Cambridge, 1973)
4. S. Boettcher, *Numerical Results for Ground States of Spin Glasses on Random Graphs,* in preparation
5. L. Viana, A.J. Bray, J. Phys. C **18**, 3037 (1985)

6. M. Mézard, G. Parisi, M.A. Virasoro, *Spin Glass Theory and Beyond,* (World Scientific, Singapore, 1987)
7. M. Mézard, G. Parisi, Eur. Phys. J. B **20**, 217 (2001)
8. G. Parisi, F. Tria, Eur. Phys. J. B **30**, 533 (2002)
9. M. Mézard, G. Parisi, Europhys. Lett. **3**, 1067 (1987)
10. P. Mottishaw, Europhys. Lett. **4**, 333 (1987)
11. P.-Y. Lai, Y.Y. Goldschmidt, J. Phys. A **23**, 3329 (1990)
12. C. De Dominicis, Y.Y. Goldschmidt, J. Phys. A **22**, L775 (1989)
13. Y.Y. Goldschmidt, C. De Dominicis, Phys. Rev. B **41**, 2184 (1989)
14. M. Mézard, G. Parisi and R. Zecchina, Science **297**, 812 (2002)
15. R. Monasson, R. Zecchina, S. Kirkpatrick, B. Selman, L. Troyansky, Nature **400**, 133 (1999), and Random Struct. Alg. **15**, 414 (1999)
16. F. Ricci-Tersenghi, M. Weigt, R. Zecchina, Phys. Rev. E **63**, 026702 (2001)
17. S. Franz, M. Leone, F. Ricci-Tersenghi, R. Zecchina R, Phys. Rev. Lett. **87**, 7209 (2001)
18. K.Y.M. Wong, D. Sherrington, J. Phys. A **20**, L793 (1987)
19. J.R. Banavar, D. Sherrington, N. Sourlas, J. Phys. A **20**, L1 (1987)
20. S. Boettcher, A.G. Percus, Artificial Intelligence **119**, 275 (2000)
21. S. Boettcher, A.G. Percus, Phys. Rev. Lett. **86**, 5211 (2001)
22. M.R. Garey, D.S. Johnson, *Computers and Intractability, A Guide to the Theory of NP-Completeness* (W.H. Freeman, New York, 1979)
23. T. Klotz, S. Kobe, J. Phys. A **27**, L95 (1994)
24. R.G. Palmer, J. Adler, Int. J. Mod. Phys. C **10**, 667 (1999)
25. C. Desimone, M. Diehl, M. Jünger, P. Mutzel, G. Reinelt, G. Rinaldi, J. Stat. Phys. **80**, 487 (1995)
26. F. Liers, M. Junger, Int. J. Mod. Phys. C **11**, 589 (2000)
27. K.F. Pal, Physica A **223**, 283 (1996); **233**, 60 (1996)
28. A.K. Hartmann, Phys. Rev. B **59**, 3617 (1999); Phys. Rev. E **60**, 5135 (1999)
29. J. Houdayer, O.C. Martin, Phys. Rev. Lett. **83**, 1030 (1999)
30. S. Boettcher, M. Grigni, G. Istrate, A.G. Percus, *Extremal Optimization at the Phase Transition of the 3-Coloring Problem,* in preparation
31. S. Boettcher, J. Math. Phys. A **32**, 5201 (1999)
32. S. Boettcher, A.G. Percus, Phys. Rev. E **64**, 026114 (2001)
33. S. Boettcher, *Numerical Results for Ground States of Mean-Field Spin Glasses at low Connectivities,* `cond-mat/0208444`
34. S. Boettcher, Comput. Science Engineering **2**, 75 (2000)
35. S. Boettcher, M. Grigni, J. Phys. A **35**, 1109 (2002)
36. A.K. Hartmann, Phys. Rev. E **63**, 016106 (2001)
37. *7th DIMACS Implementation Challenge on Semidefinite and related Optimization Problems,* edited by D.S. Johnson, G. Pataki, F. Alizadeh (to appear, see `http://dimacs.rutgers.edu/Challenges/Seventh/`)
38. F. Liers, private communication
39. D. Dean, Eur. Phys. J. B **15**, 493 (2000)
40. M. Mézard, private communication
41. P. Sibani, J.C. Schoen, P. Salamon, J.O. Andersson, Europhys. Lett. **22**, 479 (1993); T. Klotz, S. Schubert, K.-H. Hoffmann, Eur. Phys. J. B **2**, 313 (1998)
42. D. Sherrington, S. Kirkpatrick, Phys. Rev. Lett. **35**, 1792 (1975)
43. I. Kanter, H. Sompolinsky, Phys. Rev. Lett. **58**, 164 (1987)